DACOMAT

Deliverable number: D3.4

Report on the mixed mode interface cohesive laws using a new test method

Peter Jenkins (University of Strathclyde)

Bent F. Sørensen, Stergios Goutianos and Daan Cederløf (DTU)

The DACOMAT project has received funding from the European Union's Horizon 2020 research and innovation programme under GA No. 761072

Deliverable details

Document name: development of a new test to investigate mixed mode interface cohesive laws at the microscale

Responsible partner: UNIS

Work package: WP3

Task: 3.1: Micromechanical testing

Due date: 30.06.2019

Extended due date: 31.12.2019

Delivery date: 27.10.2020

Dissemination level	
X	PU = Public
	CO = Confidential, only for members of the consortium (including the EC)
	Classified, information as referred to in Commission Decision 2001/844/EC.
Deliverable type	
X	R: Document, report (excluding the periodic and final reports)
	DEM: Demonstrator, pilot, prototype, plan designs
	DEC: Websites, patents filing, press & media actions, videos, etc.
	OTHER: Software, technical diagram, etc.

Disclaimer:
The information in this document reflects the views only of the author, and the Commission cannot be held responsible for any use which may be made of the information contained therein.

The DACOMAT project has received funding from the European Union's Horizon 2020 research and innovation programme under GA No. 761072

Contents

The DACOMAT project has received funding from the European Union's Horizon 2020 research and innovation programme under GA No. 761072

1.Introduction

1.1 Motivation

Composite materials are used increasingly in a huge variety of engineered parts, across global sectors such as transport, energy and construction. They offer numerous advantages over more traditional materials, for example excellent strength and stiffness to weight rations, natural resistance to corrosion and the ability to be formed into complex shapes using a wide range of manufacturing techniques. The success of any composite is reliant on a number of factors, such as appropriate design and choice of materials. Another critical factor, perhaps the most important, is an effective interface between matrix and reinforcement material. Without an effective interface the various phases of a composite part will not yield the desired properties based on their combination.

In modern fibre reinforced polymer composites, a successful interface is created by tailoring the correct polymer with fibres which have the appropriate surface coating, known as sizing. Although it is integral to the production of an effective composite, the precise nature and performance of the interface, or interphase region more generally, is not fully understood. Small changes, for example to the resin or fibre sizing, can have significant consequences on interfacial performance. A common way to quantify the interfacial performance is through measurements of adhesion. This expression encompasses a number of possible mechanisms which may be at play in the formation of the interface, or more generally interphase region, such as direct chemical bonding, residual stresses, mechanical interlocking and friction.

A number of tests exist to measure adhesion, one class of which are micromechanical test methods. These have a number of key advantages. They generally simplify the analysis by considering, for example, interaction between a given volume of matrix and a single fibre. The micro-scale of the samples also means manufacture of samples is quicker than other macro-tests and consumes significantly less raw materials. Four common micromechanical tests for measurement of fibre-matrix adhesion have been utilised in the literature: single fibre fragmentation, microbond (micro droplet debond), fibre pull out and fibre push out. They possess various advantages and disadvantages in comparison with one another, however, all of these methods produce similar type failures: loading is always applied parallel to the fibre direction, therefore a mode II shear failure occurs.

The failure of a ‘real-life’ composite parts is, however, far more complicated than any of these micromechanical representations, although it will be at least partly comprised of shearing failure of the matrix at the interface with fibres. In the context of the DACOMAT project and its goals, improving the understanding of the interfacial adhesion between fibres and resins is of significant importance. The bridging of fibres utilised to arrest crack growth means they experience complex stresses at various angles to their longitudinal axis. Fibre breakage is possible, but if there is an interfacial failure in a crack bridging fibre it will not be well approximated by the mode II micromechanical tests commonly used.

1.2 Purpose

The purpose of this work is to demonstrate the development of a new micromechanical interface test. This test will be capable of generating data on the mixed mode failure of the fibre-matrix interface at the micro scale. The information contained within this report summarises the developmental work involved in creating this test; however, it is not a final summary of all developments as further evolvement of the test over time is inevitable.

The DACOMAT project has received funding from the European Union's Horizon 2020 research and innovation programme under GA No. 761072

2.Background

2.1 Micro-mechanical tests for interfacial strength measurement

Four common micromechanical tests for measurement of fibre-matrix adhesion have been described and utilised in the literature: single fibre fragmentation, microbond (micro droplet debond), fibre pull out and fibre push out. They possess various advantages and disadvantages in comparison with one another, however, all of these methods produce similar type failures: loading is always applied parallel to the fibre direction, therefore a mode II shear failure occurs. Representations of these test methods are shown in Figure 1.

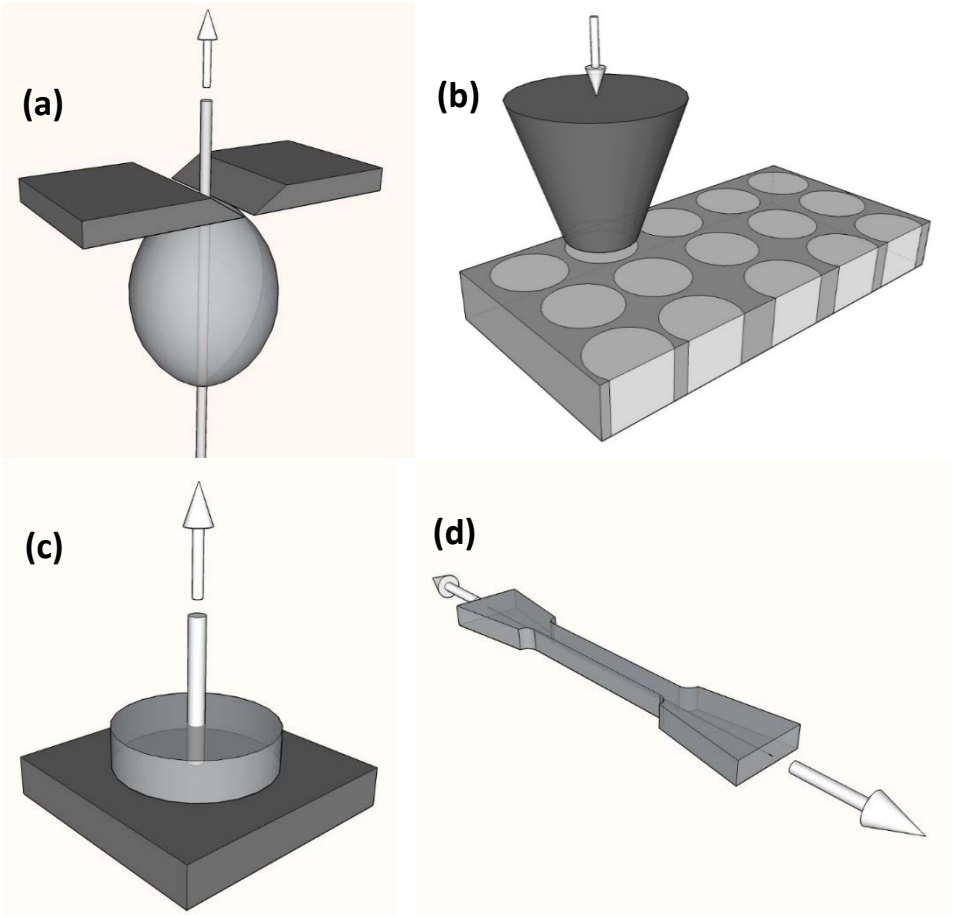

Figure 1: representations of the micro scale interface testing methods: (a) microbond (b) fibre push out (c) fibre pull out (d) single fibre fragmentation test

These tests generate similar data regarding interfacial adhesion in the form of the interfacial shear strength (IFSS). It is possible to gain further insights using a special form of single fibre fragmentation test [1]. All of these test methods, however, have been critiqued by authors such as Piggott [2,3]; his assertion is that the centro-symmetric form of failure in such tests is unrealistic and may be significantly influenced by factors such as fibre surface roughness and cure shrinkage during sample manufacture.

The DACOMAT project has received funding from the European Union's Horizon 2020 research and innovation programme under GA No. 761072

2.2 Existing fibre peel micro-mechanical tests

As a response to this criticism of the current (at that time) state of the art in micromechanical testing, Piggott and colleagues researched and developed an alternative method to measure interfacial adhesion of samples at the single fibre scale. They drew inspiration from the established field of peel testing, which is governed by numerous standards when working with common macro scale samples (for example ASTM 1876-08, ASTM 1781-98). They developed methods of sample production for reinforcement fibres of diameters as small as 8 µm and a testing process for variable peeling angles [4–6]. This technique did not, apparently, garner significant interest from other research groups and there is no evidence in the literature that it has been used by researchers in 15 years or more.

3.Experimental

3.1 Materials

The ultimate target is to perform both versions of the single fibre peel test with commonly used continuous glass fibres with diameters in the approximate range 15-20 µm. Initially, however, two additional types of fibres of larger diameter were used. These fibres are significantly easier to work with during test development.

Commercially available SE3030 boron-free E-glass fibres were obtained from 3B-fibreglass. They were supplied as single-end continuous direct rovings; a multi-functional size designed for compatibility with thermoset resins was applied during manufacture from aqueous solution by a high-speed contact roller. Packages were dried for 24 hours to remove residual moisture. The nominal diameter of the fibres was 17 µm. Thick E-glass fibres with no surface sizing (unsized) were produced on a pilot scale bushing at the Aachen Institute of Textile Technology. Fibres were cooled immediately after fibrisation using a water spray and were then wound onto cardboard tubes; their nominal diameter was 35 µm. Stainless steel wire AISI 302 with nominal diameter of 50 µm was purchased from Goodfellow.

Two different resins were used during development of the single fibre peel test. The vinyl ester resin DION VE-1260 produced by Polynt was selected; the standard initiator Norox PBC-21 was used. They were mixed at a ratio of 97.5:2.5 by weight. A second epoxy-based resin was also chosen, due to its significantly shorter cycle time for the preparation of samples. The Bisphenol A diglycidyl ether epoxy resin DER 332 was sourced from Sigma Aldrich, as was the curing agent triethylenetetramine. They were mixed at the stoichiometric ratio.

The method developed to prepare test specimens was to spread resin across the surface of a tab of dimensions 76x26 mm (size of a standard microscope slide). Two substrate materials were used: standard glass microscopy slides and fully opaque black PMMA sheet. The PMMA sheet was cut to the required dimensions using a laser cutter.

3.2 Sample preparation

The method of sample preparation developed deviates significantly from that described in previously published studies, in which small capsules were filled with resin [4,5]. The vinyl ester resins utilised in the DACOMAT project undergo significant shrinkage during the curing the process; therefore, the surface of the resin would recede below the capsule's edge making controlled imbedding of fibres all but impossible. The alternative method employed was to spread resin across the surface of a flat

The DACOMAT project has received funding from the European Union's Horizon 2020 research and innovation programme under GA No. 761072

substrate. The dimensions selected were 76x26 mm, the dimensions of a standard microscope slide, as this was compatible with commercially available spin coating equipment.

3.2.1 Resin distribution by spin coating

Spin coating was performed using a Laurell WS-650-23 Spin Coater; this was predominantly used for the spreading of vinyl ester resin. The viscosity of DER332 epoxy resin mixed at stoichiometric ratio is higher than that of vinyl ester, therefore it is not possible to achieve the same evenness of coating by spinning this resin. Nonetheless, epoxy samples were prepared using this method. The following steps describe the method.

1. A clean slide was placed into the coater and secured in place using the vacuum
2. Approximately 1.0 ml of freshly mixed resin was added to the centre of the slide using a syringe
3. The lid was closed securely and the program initiated
4. During the first 10 seconds the machine accelerated up to the set rotational speed
5. Once this speed was achieved spinning was performed for either 30 or 50 seconds
6. Once complete the machine decelerated to zero within 2-3 seconds
7. The sample was removed and set aside; one or more fibres were placed manually on the resin coated surface within 1 minute of cessation of spinning
8. The samples were cured following the required cure schedule:
    a. Vinyl ester: 24h under vacuum at room temperature followed by post-cure process in air of 24h at 60 °C, 3h at 80 °C and 1h at 100 °C
    b. Epoxy: 1h at 60°C then 2h at 120 °C with heating ramp rate of 2 °C/min, under air

An example of a sample produced using spin coating is shown in Figure 2. The significant variables in the process were the rotational speed and the time for which this speed was maintained. It was found that time at maximum speed did not have a large effect on the spreading of the resin or thickness achieved. It can be seen at the right hand edge of the sample shown in Figure 2 that resin did not reach the extreme edges. A spinning time of 30 seconds is therefore recommended.

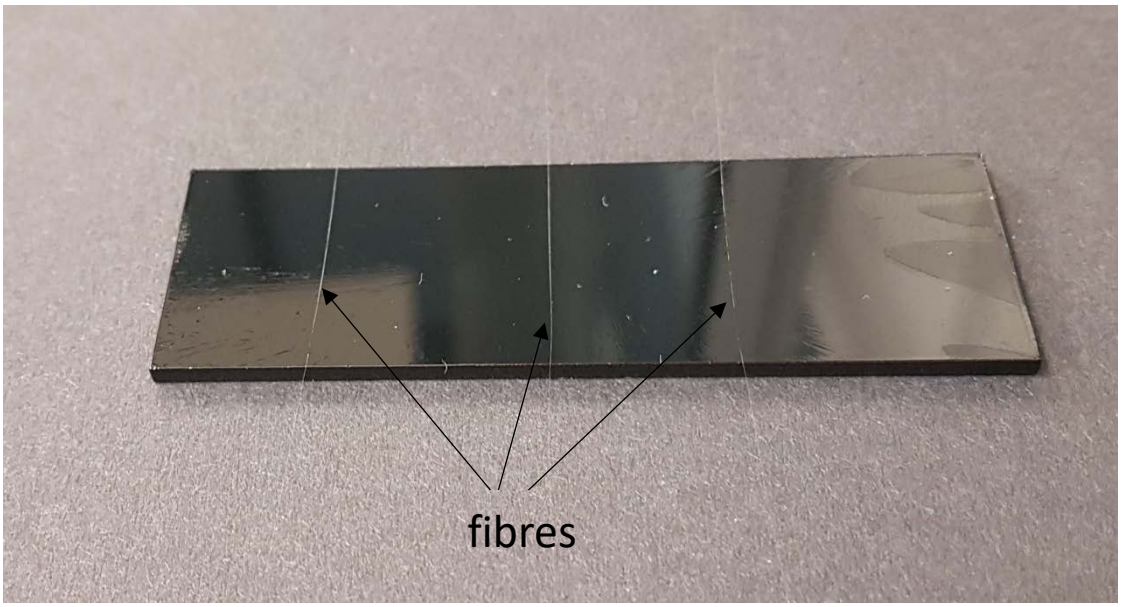

Figure 2: image showing a PMMA slide spun coated with vinyl ester resin and 3 fibres attached

Increasing the rotational speed of the coating process had a more significant effect on the efficacy of resin spreading. A maximum speed of 9000 rpm was selected. The thickness of resin layer achieved was assessed using a micrometer: several points on a clean slide were measured before and after

The DACOMAT project has received funding from the European Union's Horizon 2020 research and innovation programme under GA No. 761072

spin coating with VE-1260. The layer thickness achieved at 9000 rpm for 30s was approximately 10 µm.

3.2.2 Resin distribution by rolling

To disperse more viscous resin (e.g. epoxy) over the surface of slides an alternative mechanical method was necessary. The following procedure was established.

1. Add several ml of mixed resin to one end of a slide
2. Using a silicon roller, spread the resin across the surface until a sufficiently even coverage was achieved
3. Place the tab to one side for a period of time to allow gelation of the resin to occur
4. After a suitable gelation period, place fibres on the surface of the sample tab
5. Cure the resin by following the cure schedule described above

This procedure is more complex and less efficient than spin coating as samples must be left to gel for a significant time before fibres can be added and the cure cycle initiated. There is also much greater potential for over-embedding of fibres, as they will sink into the resin if insufficient time for gelation is given. For this reason, spin coating was preferred where possible.

3.3 Analysis and test setup Strathclyde

3.3.1 Equipment

A Leitz Ergolux optical microscope was used for direct examination of samples and measurement of fibre diameters at 200-500x magnification. The samples were imaged at 90° to the surface of the resin using reflected light. A small amount of imaging was carried out using Hitachi SU-6600 Field Emission Scanning Electron Microscope. Samples were sputter coated with gold and an accelerating voltage of 5kV was used.

Profilometry data were obtained using a Mitutoyo Surftest SJ-2000 stylus profilometer. The scan speed was 0.02 mm/s and the detector force was 0.75 mN. Raw 2-dimensional line scan data were exported into Origin for analysis. It is possible to scan samples either pre- or post- fibre peel test.

The single fibre peel test was conducted using a Testometric M250-2.5CT tensile machine equipped with a 5 N load cell. Tests for which data are presented in this report were carried out at a peel angle of 30° or 90° and the column extension rate was 1 mm/min. Future tests will be performed at 60 and 45° to the sample surface. Fibres were clamped directly using the machine grips which are rubber surfaced and pneumatically operated. This is a significant advantage over the use of slip foils and adhesives due to the time saved during testing.

3.3.2 Determination of fracture energy release rate

The equations to calculate the fracture energy release rate of the fibre-matrix interface G_c^i in a peel test configuration were developed by Alimuddin and Piggott [4] for both the normal case and for oblique angles of peeling. For a fibre half-embedded and peeled normal to the surface, the fracture energy release rate is a function of average debonding force, over a given length and fibre diameter, d.

$$G_I^c = \frac{\bar{F}}{2\pi d} \qquad \text{(Eq. 1)}$$

The DACOMAT project has received funding from the European Union's Horizon 2020 research and innovation programme under GA No. 761072

For peeling of fibres at an oblique angle less than 90°, a correction factor must be applied to account for the difference between peeled length in the angled plane direction and displacement of the tensile column in the vertical direction. If the peel angle is defined as ϕ then fracture energy release rate is given by Eq. 2.

$$G_I^c = \frac{\bar{F}(1 - cos\varphi)}{2\pi d} \quad \text{(Eq. 2)}$$

3.3.3 Determination of degree of fibre embedding

3.3.3.1 Visual methods

To visually assess the degree to which a fibre sample is embedded in the surrounding matrix resin it is necessary to measure with sufficient accuracy both the fibre diameter and the interface with the resin along both sides of its length. Two visual observation techniques were attempted, electron and optical microscopy. Once these values are obtained the embedded perimeter P_{ebd} of the fibre may be calculated as shown in Figure 3 and Eq. 3 and 4.

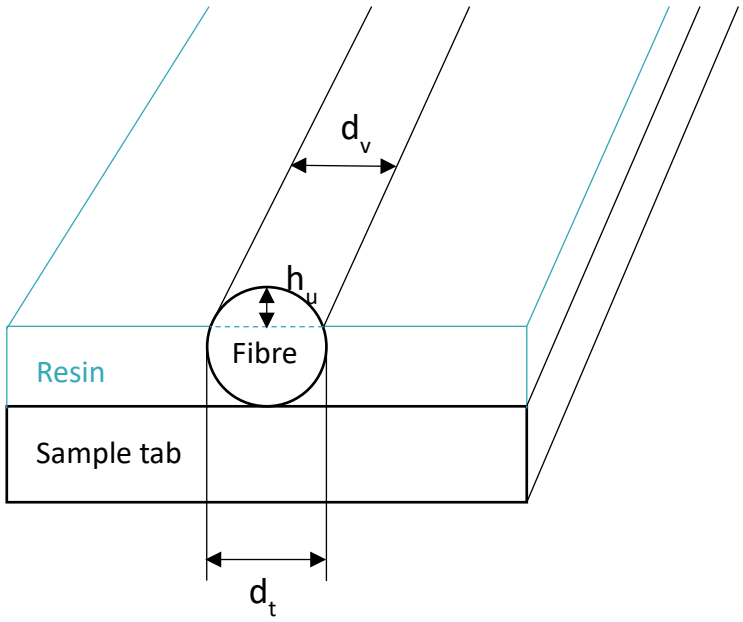

Figure 3: fibre peel sample measurements required for calculation of embedded depth & perimeter

$$h_u = \frac{d}{2} - \sqrt{\frac{d^2}{2} - \frac{d_v^2}{2}} \quad \text{(Eq. 3)}$$

$$P_{ebd} = (100\%) \times \frac{d - h_u}{d} \quad \text{(Eq. 4)}$$

In the equations d_v is the visible portion of the fibre looking at right angles to the sample surface, h_u is the height of the fibre portion above the resin surface and P_{ebd} is the perimeter of the fibre that is embedded.

The DACOMAT project has received funding from the European Union's Horizon 2020 research and innovation programme under GA No. 761072

In practice, however, there are significant challenges in applying this methodology whether optical or scanning electron microscopy is used. When using optical microscopy there is a trade-off between image quality, image size, depth of field and speed of imaging. A compromise was found using a magnification of 200x. Features and dimensions can be resolved reasonably well, and the analysis speed is acceptable. A typical image is shown in Figure 4.

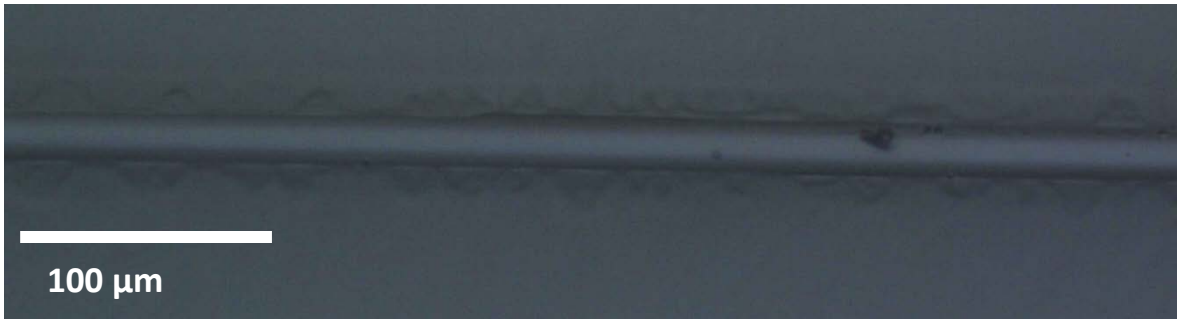

Figure 4: 200x magnification optical microscopy image of glass fibre embedded in vinyl ester resin (spin coating)

This image illustrates the challenges encountered when attempting to define the interface between fibre and resin for the purposes of measuring the interfacial area based on optical microscopy images. There is some fluctuation along the fibre length but it is difficult to observe precisely. This fibre is around 50 % embedded along the section shown in Figure 4.

Some trial images were captured using SEM. An example of the type of image obtained is given in Figure 5. Excellent clarity can be achieved, including the tricky interface region between the fibre and surrounding resin.

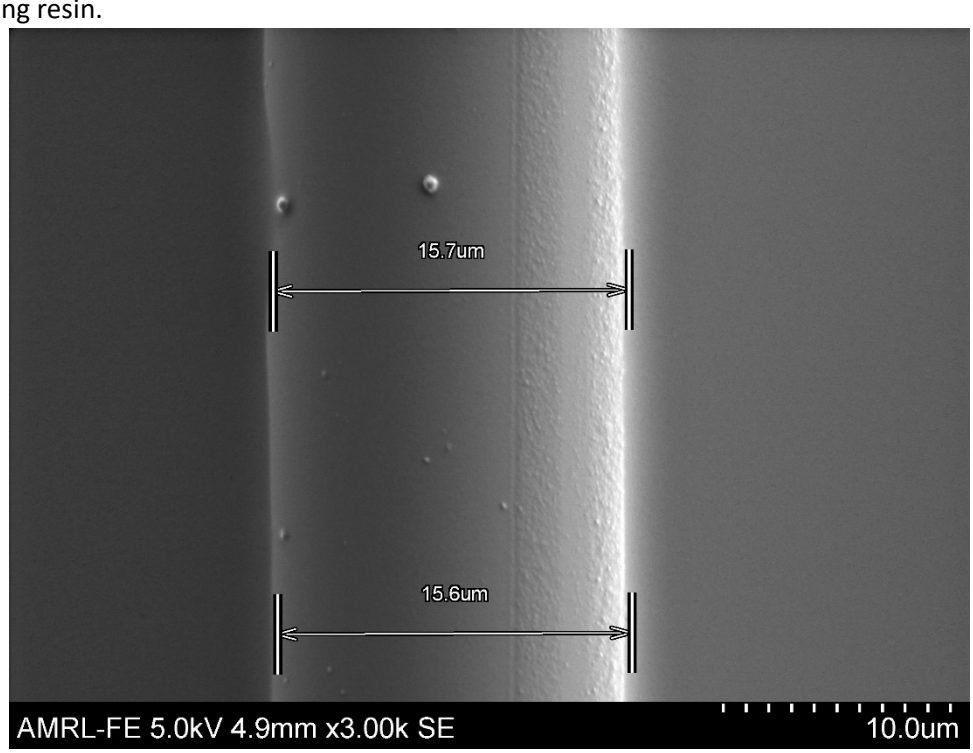

Figure 5: 3000x magnification SEM image of glass fibre embedded in vinyl ester resin (spin coating)

In this example the full fibre diameter was 18.5 µm so the portion of fibre shown was embedded to 76-77 % of its perimeter. SEM observation of samples is relatively time consuming. Images at high magnification give more detail about the interface but each image shows only a tiny fraction of the

The DACOMAT project has received funding from the European Union's Horizon 2020 research and innovation programme under GA No. 761072

full fibre. For example, the length of fibre sections shown in Figure 5 is approximately 30 µm, whilst the debond energy data may be collected over a length at least 100 times greater.

3.3.3.2 Physical methods

In addition to visual methods, physical imaging of samples was investigated using a stylus profilometer. It is possible to measure sample profiles either before or after testing, and there are advantages and disadvantages to each approach. A typical profile of a sample after fibre debond is shown in Figure 6. A clear depression is left in the resin, the edges of which can be identified more easily using a finer scale. A simple measurement tool in Origin can then be used to find the length: in conjunction with the fibre diameter these data can be used to calculate the degree of fibre embedding in similar manner to the technique described in Eqn. 3 and 4. In the example in Figure 6 the distance from edge to edge was about 27 µm; therefore the fibre was only approximately 20% embedded.

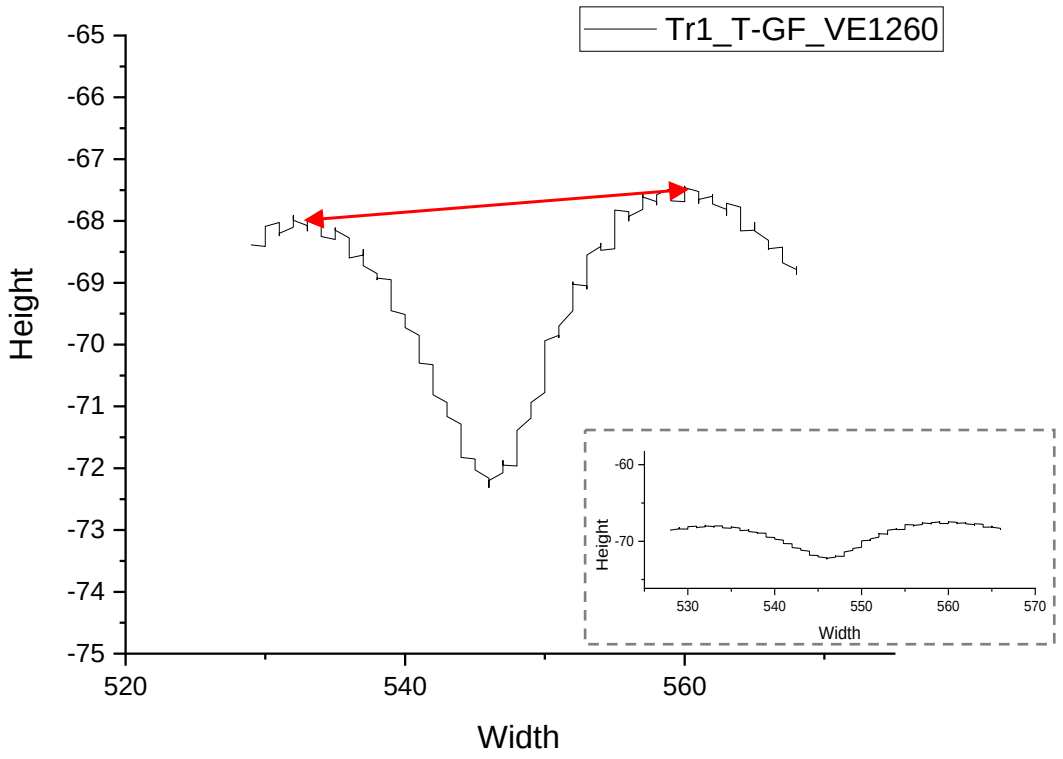

Figure 6: typical profilometry data of thick glass fibre (diameter approx. 34 µm) after fibre debonding. Inset (dotted line) shows 'true' proportions of the profile on equally scaled x and y axes

The DACOMAT project has received funding from the European Union's Horizon 2020 research and innovation programme under GA No. 761072

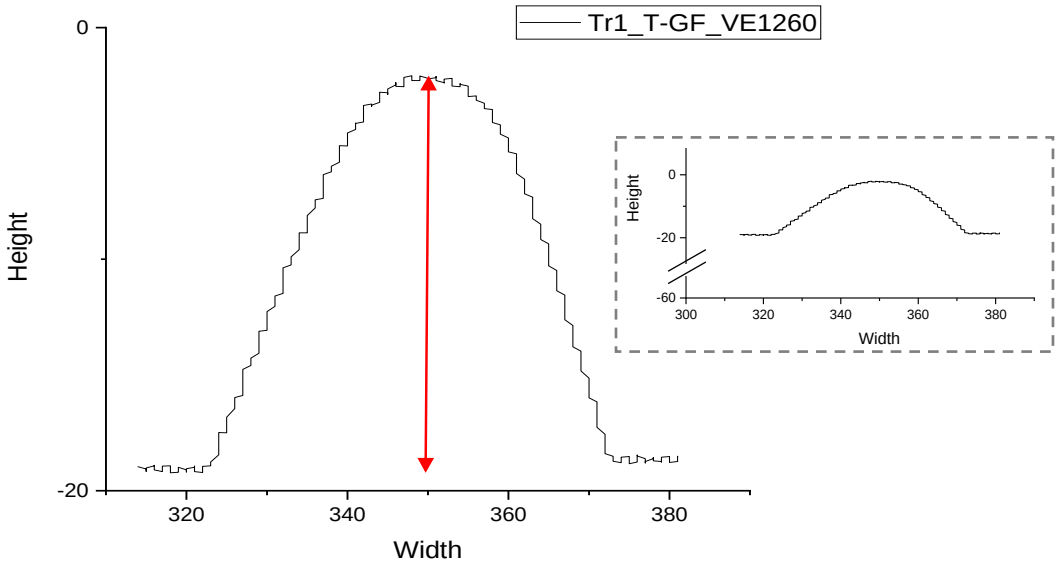

Figure 7: typical profilometry data of thick glass fibre (diameter approx. 34 µm) before fibre debonding. Inset (dotted line) shows 'true' proportions of the profile on equally scaled x and y axes

Figure 7 shows a profile obtained for a fibre prior to testing. The height above the flat resin surface for this sample was measured at 16.9 µm, suggesting very close to 50% embedding. An issue arises, however, with the apparent width of the protrusion; in the example shown in Figure 7 the data suggest a total width of approximately 50 µm. It is likely that the stylus may have insufficient resolution to accurately measure the fibre in its lateral direction of travel: the edge bumps against the fibre before the tip is in place to resolve the outline properly, producing a widening of the feature. However, it should be possible to use the height data alone in conjunction with an accurate measurement of fibre diameter.

Whether the profile is measured before or after debond, the same data are required: fibre diameter (probably measured optically) and a height profile. In this case, it may be more efficient to measure the profile after debonding. This way, the profiles can be obtained in the region of interest only (where the fibre aligned straight with the tensile column and maintained the desired testing angle). Another advantage is that the stylus applies a small force when scanning the surface, and the possible effect of this on a fibre yet to be tested is unknown and, potentially, would be hard to quantify. The small force applied may move the fibre, causing a change in the measured adhesion. This issue does not arise if scanning is done post-test. The most notable disadvantage of post-test measurement is that the edges of the depression left by a debonded fibre are more difficult to accurately delineate than the height difference between the resin plane and top of the fibre. This will slightly lengthen the analysis time required.

3.3.4 Testing fixture design

It is known that the average peel force is a function of the peel angle used, therefore a fixture to allow testing at multiple angles was developed. A two-part design was created: an aluminium base plate was manufactured which attached to the tensile machine using a pin and tightening nut configuration, similar to the supplied tensile machine grips. The design of the base plate is shown in Figure 8 and Figure 9.

The DACOMAT project has received funding from the European Union's Horizon 2020 research and innovation programme under GA No. 761072

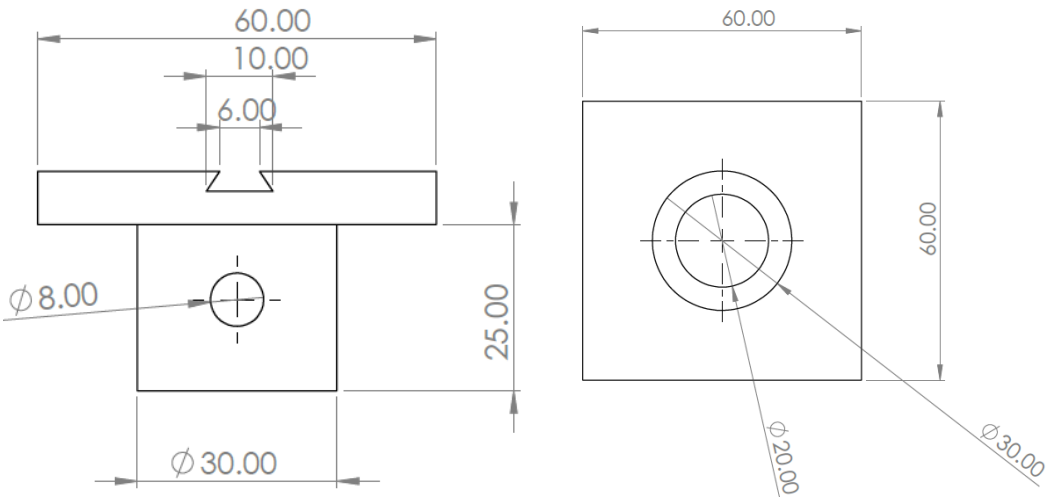

Figure 8: drawings of single fibre peel test fixture base plate

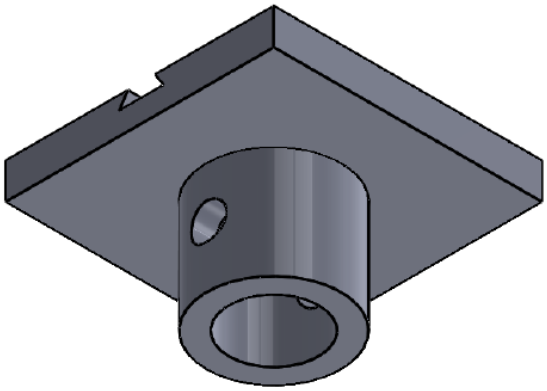

Figure 9: 3D rendered drawing of single fibre peel test fixture base plate

A dovetail was designed into the base plate; this facilitated a simple approach by which a number of fixtures at fixed angles could be used, rather than a more mechanically complex system with variable test angle. The 30° test fixture is shown in Figure 10 and Figure 11.

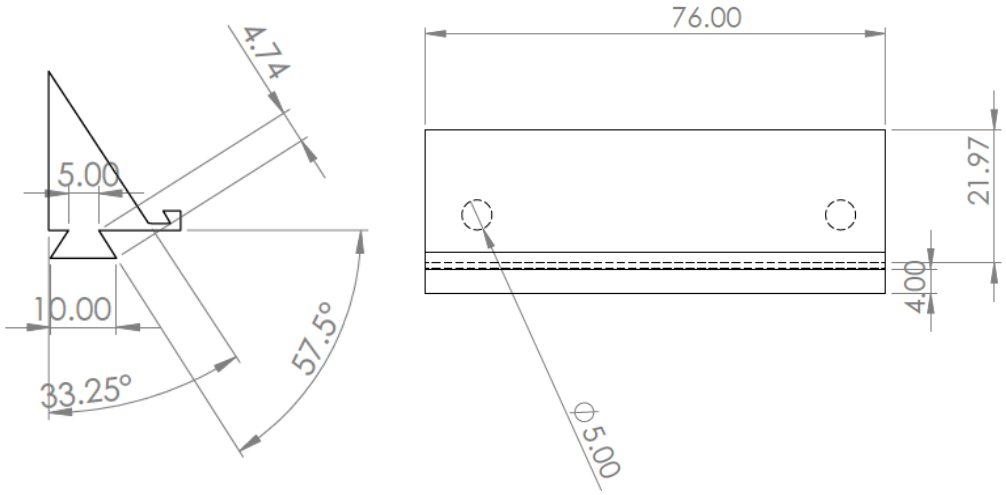

Figure 10: drawings of single fibre peel test fixture at 30°

The DACOMAT project has received funding from the European Union's Horizon 2020 research and innovation programme under GA No. 761072

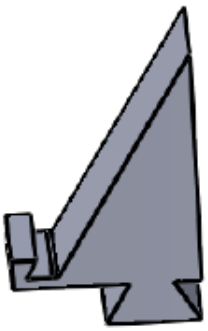

Figure 11: 3D rendered drawing of single fibre peel test fixture at 30°

The angled test fixtures were produced using a 3D printer using polylactic acid (PLA). The two 5 mm diameter hole details in the vertical face were used as securing points for simple clips, also printed using PLA, which secured the sample at the top edge of the inclined slope. An image showing the full test setup, including a mounted sample, is shown in Figure 12.

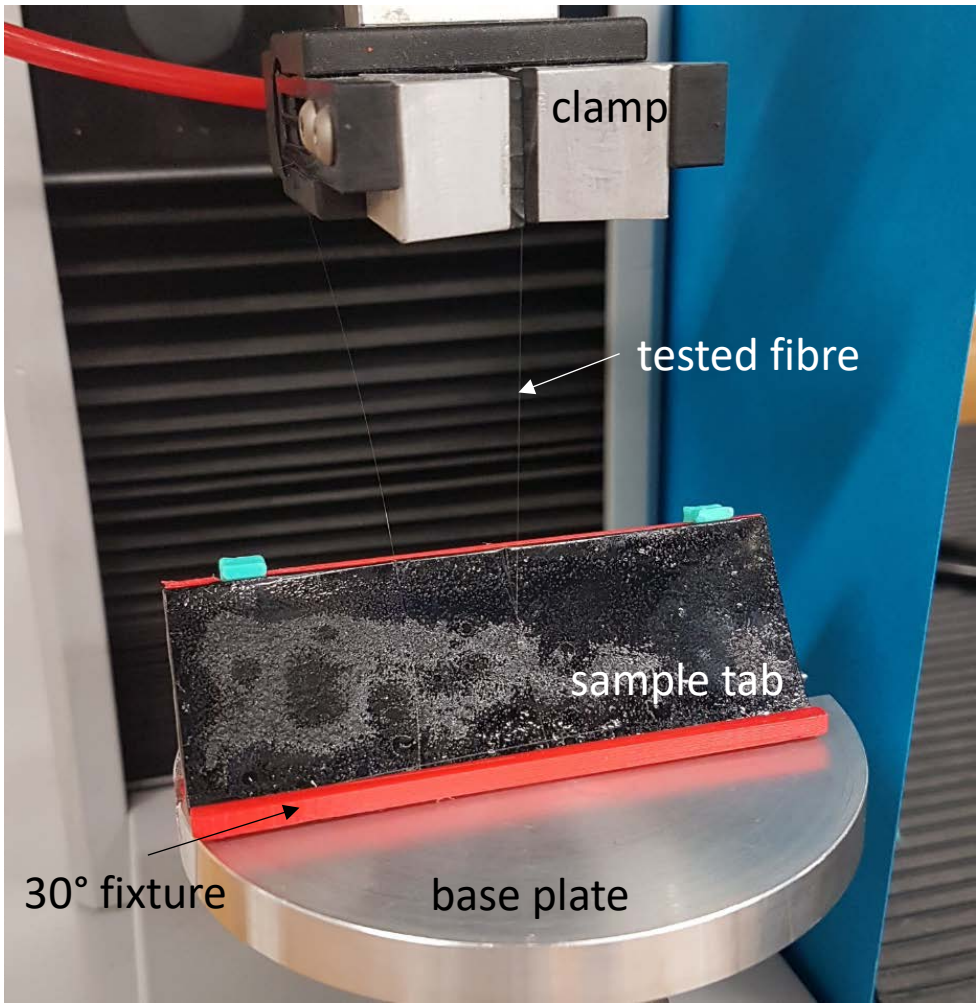

Figure 12: image showing single fibre peel test setup at 30°

The DACOMAT project has received funding from the European Union's Horizon 2020 research and innovation programme under GA No. 761072

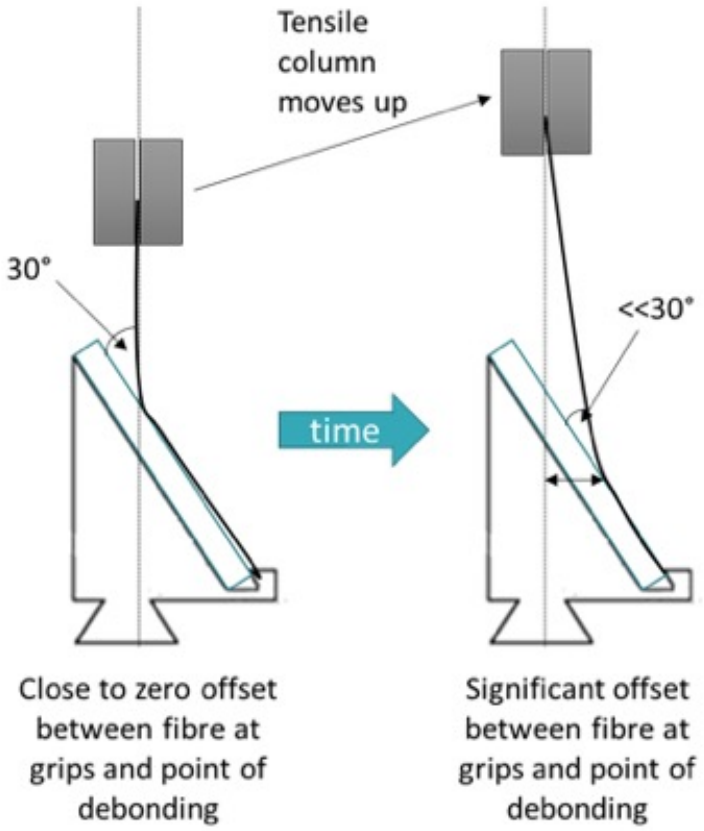

Figure 13: diagram showing change in peel angle during testing using fixed plate

Figure 13 demonstrates a consequence of using this simple fixed stage. As the machine grips are constrained to move only in the vertical direction, during testing the angle between the fibre and fixed stage changes during testing. To correct for this, data are only used from the portion of the test in which the fibre was observed to be straight in-line with the tensile column.

3.4 Analysis and test setup DTU

3.4.1 Determination of the fracture energy

In the following we set up equations that enables us to determine the fracture energy of the fibre matrix interface G_c^i by measurement of the crack tip curvature, κ.

The energy release of a beam peeling off due to a moment M is given by Toftegaard & Sørensen [7]:

$$J = \frac{M^2}{2B(EI)} \qquad \text{(Eq. 5)}$$

where B is the beam width, E is the Young's modulus of the beam and I is the moment of inertia. For a beam with a circular cross section with radius r, we have:

$$B = 2\,r \qquad \text{(Eq. 6)}$$

And

The DACOMAT project has received funding from the European Union's Horizon 2020 research and innovation programme under GA No. 761072

$$I = \frac{\pi}{4} r^4 \quad \text{(Eq. 7)}$$

Moreover, the relationship between moment M and curvature κ is given by classic beam theory:

$$k = \frac{M}{EI} \quad \text{(Eq. 8)}$$

We now set up an energy balance: The energy released during a small crack extension da, is available for consummation of the new fracture area:

$$J\ B\ da = \mathrm{G}\ \pi r\ da \quad \text{(Eq. 9)}$$

Since the beam releases energy over its full width and the fracture energy will be consumed along the semi-circle of the fibre matrix interface (the fibre is assumed to be exactly half-embedded). Inserting B from (Eq. 6) into (Eq. 9) leads to:

$$\mathrm{G} = \frac{2}{\pi} \mathrm{J} \quad \text{(Eq. 10)}$$

Inserting G from (Eq. 5) into (Eq. 10) leads to:

$$\mathrm{G} = \frac{1}{2\pi} \frac{M^2}{r(EI)} \quad \text{(Eq. 11)}$$

Then we express the moment in terms of the curvature, (Eq. 8):

$$\mathrm{G} = \frac{1}{2\pi} \frac{k^2(EI)}{r} \quad \text{(Eq. 12)}$$

Finally, we insert I from (Eq. 7) leading to:

$$\mathrm{G} = \frac{1}{8} k^2 E r^3 \quad \text{(Eq. 13)}$$

3.4.2 DTU Experimental setup and data analysis

A simplified illustration of a single fibre undergoing peeling is illustrated in Figure 14. In order to determine the radius of curvature of the fibre near the crack tip a video was taken of the peeling action inside a scanning electron microscope (SEM). A single frame obtained right before fracture occurs is used to determine the radius of curvature, from which the energy release rate is calculated as described in section 3.4.1.

The DACOMAT project has received funding from the European Union's Horizon 2020 research and innovation programme under GA No. 761072

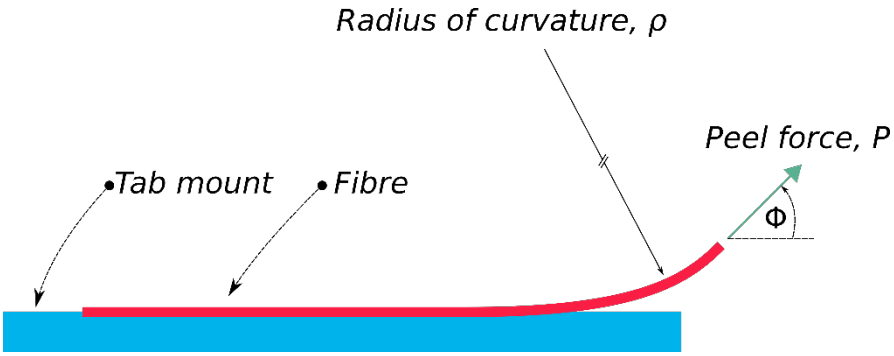

Figure 14: schematic of single fibre peeling from tab mount. (Resin layer not shown here)

A test fixture was developed to allow for in-situ scanning electron microscope (SEM) observation of a single fibre undergoing peeling. A diagram of the test fixture is shown in Figure 15. The sample tab is mounted on a fixed stage in the microscope with the loose end of the fibre mounted onto a movable stage. A stepper motor controls the travel of the movable stage such that the fibre is peeled out of the resin at a controlled rate and distance. In order to observe the fractured region where the fibre is peeled out, in addition to the curvature of the fibre (ρ), the entire setup is tilted 10 degrees.

Samples were sputter coated with approx. 7nm of gold prior to microscopy. SEM imaging was performed with a ZEISS EVO60 at an acceleration voltage of 15kV. An example of a fibre undergoing peeling is shown in Figure 16. As can be observed in Figure 16, when the fibre is peeled out, the angle of peel (Φ) increases and the radius of curvature decreases. Additionally, in the fracture region several white spots are observed, this is due to the charging of the 'fresh' resin surface which is not coated with gold.

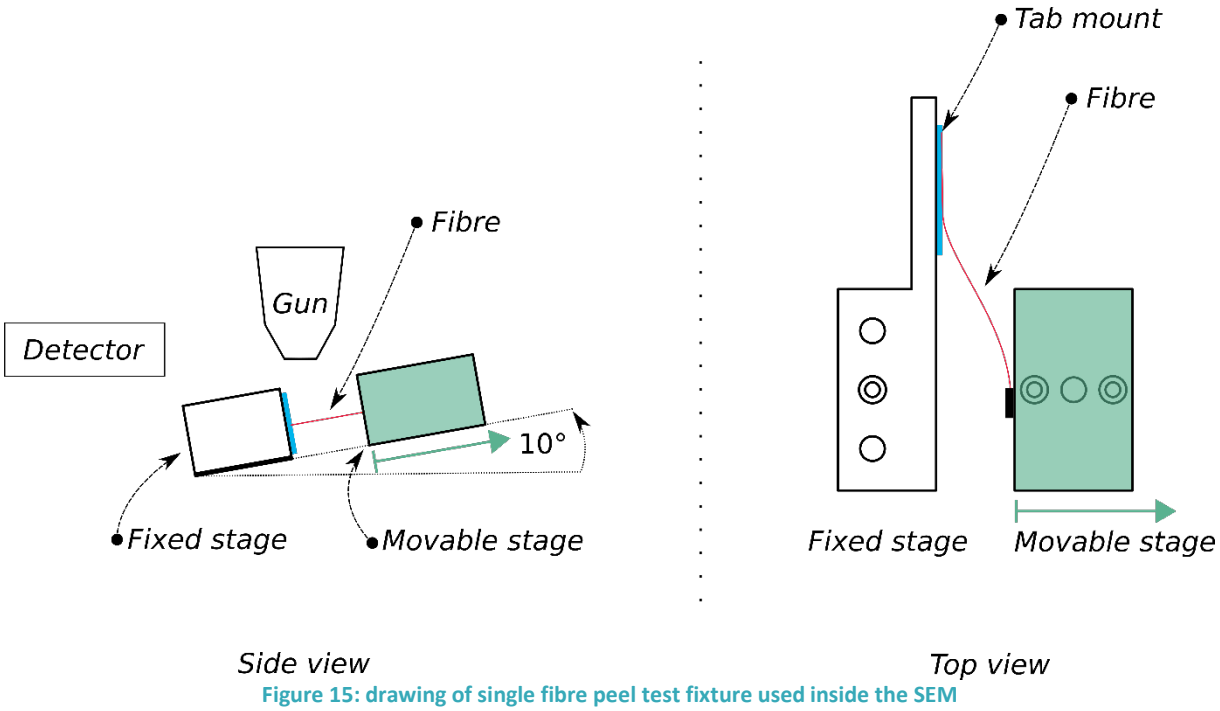

Figure 15: drawing of single fibre peel test fixture used inside the SEM

The DACOMAT project has received funding from the European Union's Horizon 2020 research and innovation programme under GA No. 761072

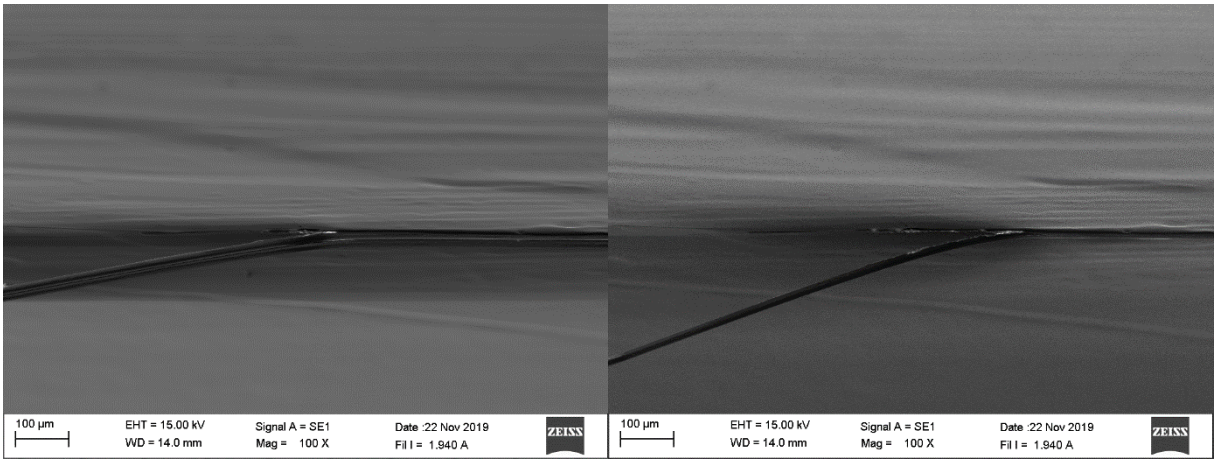

Figure 16: Progressive SEM images of the same single fibre undergoing peeling

The images obtained from the SEM video are cropped, filtered and converted to a binary image using the Matlab image processing toolbox. Of note is the adaptive foreground polarity filter within the **imbinarize** command, used to enhance the fibre edge against the dark background. Next, the free edge of the fibre (i.e. the side not embedded in the matrix as seen in Figure 17) was extracted as a series of (x,y) coordinates. This allowed for the interpolation of the curved section of the fibre (see Figure 14) using a polynomial fit in Matlab using the **cftools** function. From the fitted function the curvature k is obtained by (Eq. 14).

$$k = \frac{abs(y''(x))}{\left[1 + \left(y'(x)\right)^2\right]^{\frac{3}{2}}} \qquad \textbf{(Eq. 14)}$$

4. Experimental results

4.1 Observations

4.1.1 Sample preparation

Spin coating of fairly low viscosity resins such as vinyl ester VE-1260 allows creation of a layer of resin approximately 10 µm thick. The precise thickness is a function of the volume of resin used and the spinning parameters, although the presence of any heterogeneities on the substrate surface will also have an effect. This approximately 10 µm resin layer may be considered useful when attempting to embed typical glass fibre reinforcement fibres to half depth as they have a nominal diameter of 17 µm. Many fibres, however, will have diameters as small as 15 µm and these will typically be over-embedded using this technique. There are general concerns regarding the curing of such tiny volumes of resin with very large specific surface areas; it is easier for volatiles (for example curing agent, styrene) to evaporate which may impact proper cure. However, the surface to volume ratio of these specimens is similar to microbond droplets, which have been shown to cure sufficiently by using inert gas and elevated post cure temperatures.

Producing a thicker layer of resin, by employing a different method of resin distribution, creates a smaller specific surface area. However, it was found through experimentation that fibres placed on to this surface can easily drop beneath the surface and become fully embedded, therefore falling out with the planned geometry of test specimens. Although they can still be debonded from the resin, a portion of the energy of debonding will be due to plastic deformation of resin. Therefore, such data

The DACOMAT project has received funding from the European Union's Horizon 2020 research and innovation programme under GA No. 761072

will not be representative of the adhesion between fibre and matrix alone. Further comments on this issue are provided in 4.1.3.

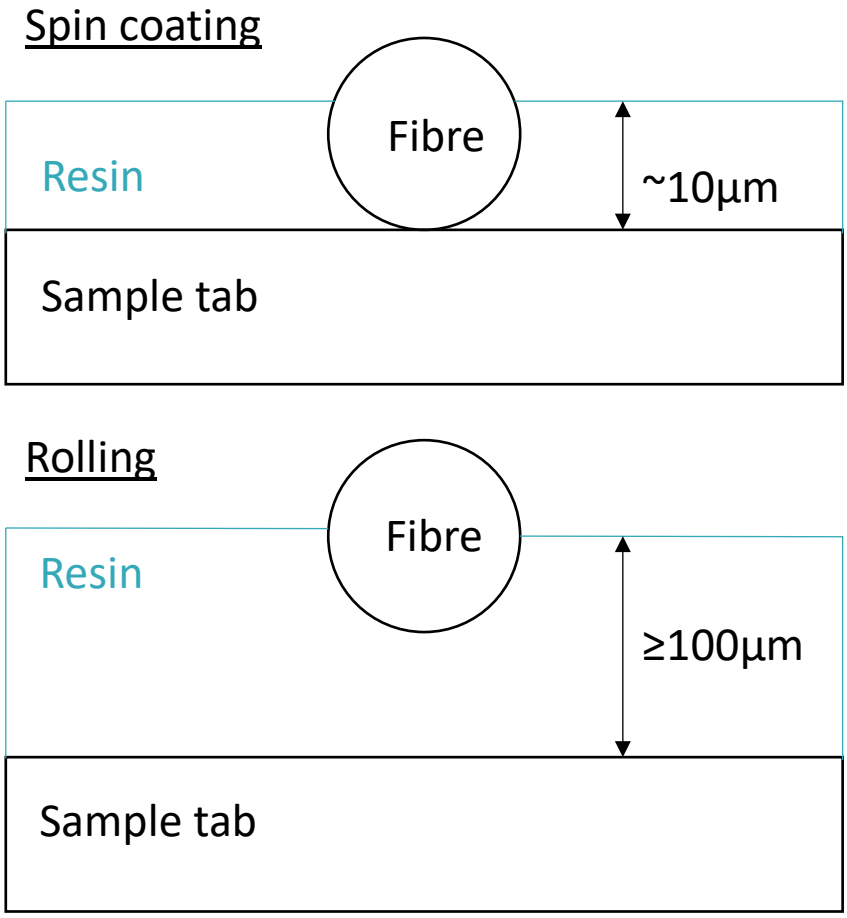

Figure 17: difference in resin thickness depending on dispersion technique used

It is necessary to allow a period of gelation to occur once the resin has been spread. If done correctly the resin will be sufficiently viscous that the fibre will not sink to become fully embedded but will be semi-embedded as desired, as shown in Figure 17. This does not generally apply to slides coated using spin coating. Standing times required for gelation have been estimated through some trial and error. For VE-1260 a standing time of 90 minutes is required when using fresh resin. For DER332 epoxy resin the standing time is approximately 1 hour. A systematic investigation of possible variation in standing times depending on the precise fibre being used has not been carried out; the simpler method of creating thin layers not requiring use of a standing time is preferred.

4.1.2 Sample observation

The challenges relating to accurate observation and measurement of the sample dimensions required for calculation of fracture energies were covered in 3.3.3. Optical microscopy does not provide sufficient clarity of the interface region between fibre and matrix, although it is the most efficient method of obtaining fibre diameters. Scanning Electron Microscopy was found to be inefficient from a time perspective due to the necessity of coating and the changeover time for each sample in the instrument.

The DACOMAT project has received funding from the European Union's Horizon 2020 research and innovation programme under GA No. 761072

Use of a physical profilometer was assessed and found to be the best compromise. Sufficient accuracy of measurement can be achieved and the time needed to take each measurement is low at around 1 minute.

An additional option is the observation of the fibre and/or the resin left behind following a successful debond by fibre peeling. Some initial using optical microscopy showed promise. It was possible to distinguish the edges of the glass fibre or the patches of resin that debonded with the fibre, as shown in the example Figure 19.

4.1.3 Over-embedding of fibres

The peel off test relies on the fibre being half-embedded or less than half-embedded. In the case that the fibre is under-embedded, the circumferential length of the bonded interface is less than πr, the energy dissipation by fibre/matrix debonding is smaller than if the fibre had been half-embedded. However, since debonding is still the only non-reversible mechanism, the experiment is still valid, but the result for the fracture energy must be corrected with a factor consisting of the nominal embedded circumferential length, πr divided by the true embedded circumferential length. This requires that both the fibre diameter and the imprint of the debonded fibre are measured.

The situation is more complicated when the fibre is over-embedded. The fibre might still be able to peel off, but in doing so the fibre now has to deform such that it can makes its way out. This will require more deformation, most likely plastic deformation and thus requires a higher force. As a result, the fibre may break. If the fibre survives, the force in the fibre was not solely due to the fibre/matrix debonding. A substantial part of the force was to deform the matrix plastically, enabling the fibre to come free. Therefore, the measurement is not valid to characterize the fibre/matrix interface. An observation of the fibre imprint would reveal if there had been substantial plastic deformation in connection with the fibre peel-off.

In real composites some bridging fibres will be over-embedded. It is interesting to consider how they would contribute to the bridging tractions. Those that survive will transmit a higher stress than those fibres that are just semi-embedded. The bridging of so-called over-embedded fibres will thus contribute positively to the crack bridging and as such increase the resulting bridging tractions.

4.2 Results from Strathclyde experiments

Initial results from the single fibre peel test have been obtained and some results are reported here. A range of samples were manufactured using one of two resins with one of three types of fibre.

- Resin: DER 332 epoxy or VE-1260 vinyl ester
- Fibre: Steel wire, thick glass fibre (unsized) or commercial SE3030 fully sized glass fibre

Trial tests were performed at a peel angle of 30° and 90°. Data are presented for a 90° peel test using SE3030 with VE-1260, comparable with data generated using the method developed at DTU and specified in 3.4. Other data were obtained using 30° peel test utilising thicker fibres with DER 332 as the embedding resin.

4.2.1 Thick glass fibre

The force-extension plot for a thick glass fibre specimen is shown in Figure 18.

The DACOMAT project has received funding from the European Union's Horizon 2020 research and innovation programme under GA No. 761072

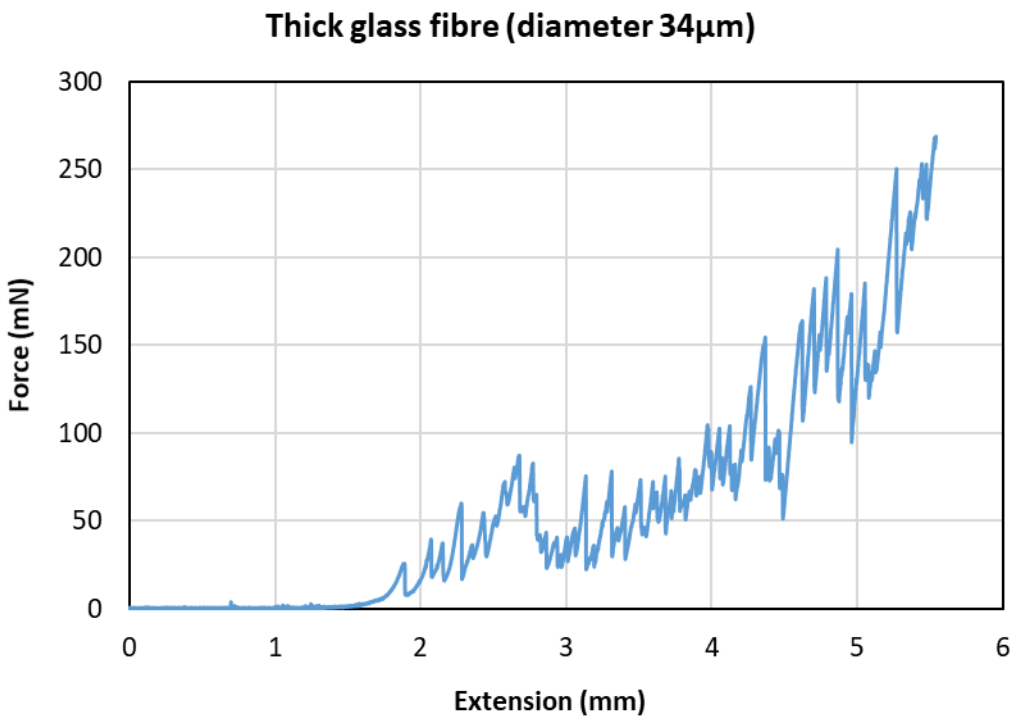

Figure 18: force-extension plot for thick glass fibre peel test at 30°

This plot shows some typical features that can occur during single fibre peel testing. There is an initial period in which slack in the fibre is taken up before it bears any load. The 'middle' portion of the test is of most interest as the useable data are found here. In this case, the fibre was observed to be parallel with the column of the tensile machine at extension of approximately 3 mm. The force data around this point, therefore, were used for analysis of the debond energy and adhesion.

It is a factor of the setup developed so far that, because the fibre is fixed at a single point, the peel angle changes slowly throughout the test. Generally, the fibre was fixed such that in the initial stages of the testing the peel angle was greater than 30°; it then passed through this point and in later stages the effective peeling angle was less than 30°. The result of this change is shown in Figure 18: as the extension increases the decrease in peel angle causes the peeling force to rise. Additionally, there may have been an increase in the embedded depth, but this was not quantified.

Due to the difficulties discussed with accurate imaging of the embedded fibre depth, an approximation was made from the images obtained. Some sample images are shown in Figure 19.

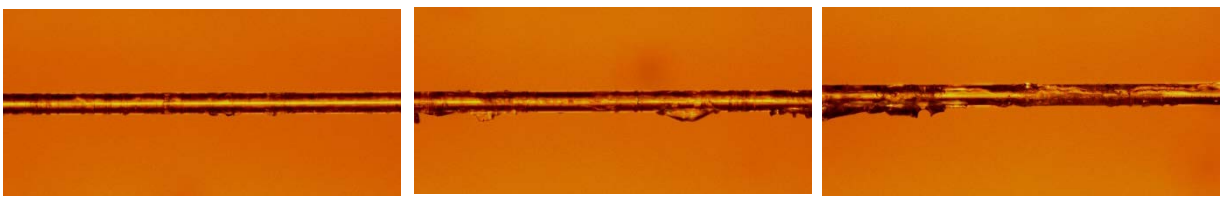

Figure 19: sample images of thick glass fibre following debonding by peel test

Some sections of the fibre were relatively clean; the fibre was estimated to be embedded in the resin to between 50-60 % depth. Other images, however, showed evidence of resin which had detached along with the fibre suggesting over-embedding.

The DACOMAT project has received funding from the European Union's Horizon 2020 research and innovation programme under GA No. 761072

A peeling angle of 30° was maintained around an extension of 3 mm in this test: the average force over the debond length 3-3.5 mm was 44.24 N. Assuming the fibre was embedded to 50% of its diameter, the debonding energy according to Eq. 2 was 27.7 J/m^2. However, in this example there remains doubt regarding the shape of the imprint left following debonding of the fibre. Residual matrix on the fibre surface effectively increases the debond length normal to the fibre longitudinal direction, likely decreasing the fracture energy.

4.2.2 Steel wire

The force-extension data for a typical steel wire sample are shown in Figure 20.

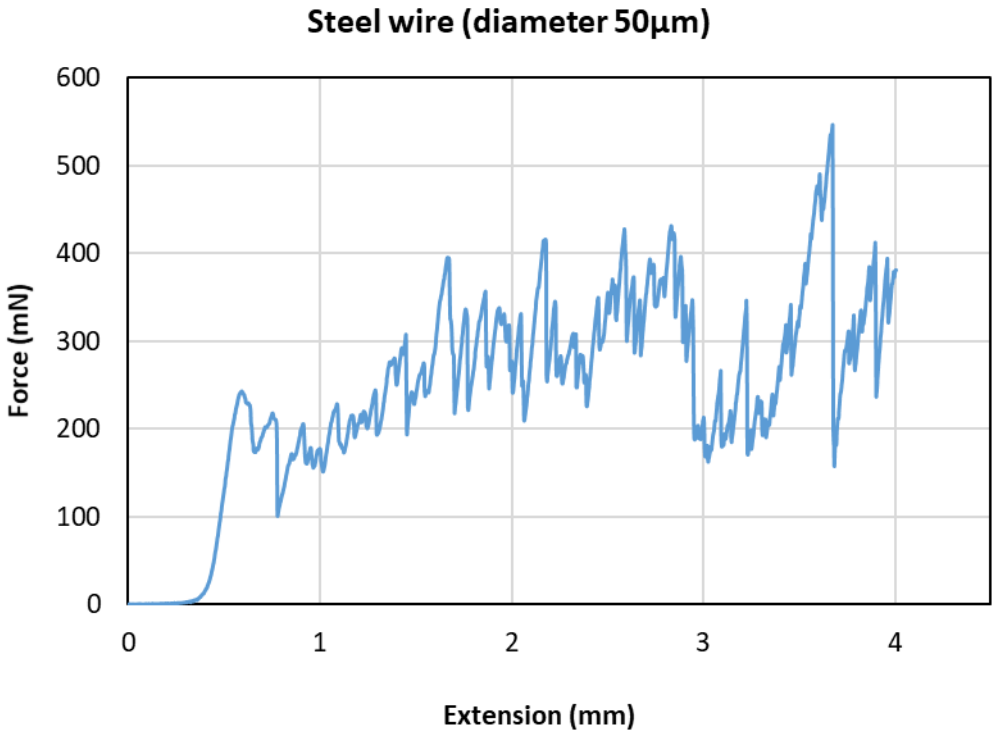

Figure 20: force-extension plot for steel wire peel test at 30°

In this case the behaviour was more stable than the thick glass fibre sample shown in Figure 18. An angle of 30° was achieved at approximately 2mm extension: the half millimetre before and after this point yield average forces of 298.2 and 295.8 mN respectively. These data are problematic, however, as the examination by microscopy strongly suggested that the steel wires were embedded too deeply within the resin. Steel wires and glass fibres were added to the partially cured resin at similar times, so this greater embedding may have simply been an effect of their higher specific gravity.

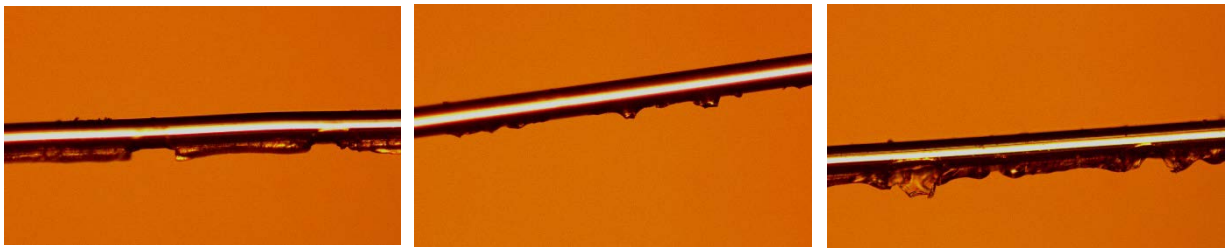

Figure 21: sample images of steel wire following debonding by peel test

The DACOMAT project has received funding from the European Union's Horizon 2020 research and innovation programme under GA No. 761072

An effect of over-embedding is shown in the sample images, Figure 21. Failure appears to have not taken place at the interface between the wire and resin; rather the matrix material has torn in the volume surrounding the fibre. The significantly greater forces during the failure are almost certainly due to the larger area over which the process took place. From measurements of the optical images, a corrected debond dimension of 63 µm was obtained. Following Eq. 2 the fracture energy release rate is approximately 100 J/m^2.

4.2.3 Commercial glass fibre

The force-extension plot for a commercially sized SE3030 fibre, embedded in VE-1260 and peeled at 90° is given in Figure 22.

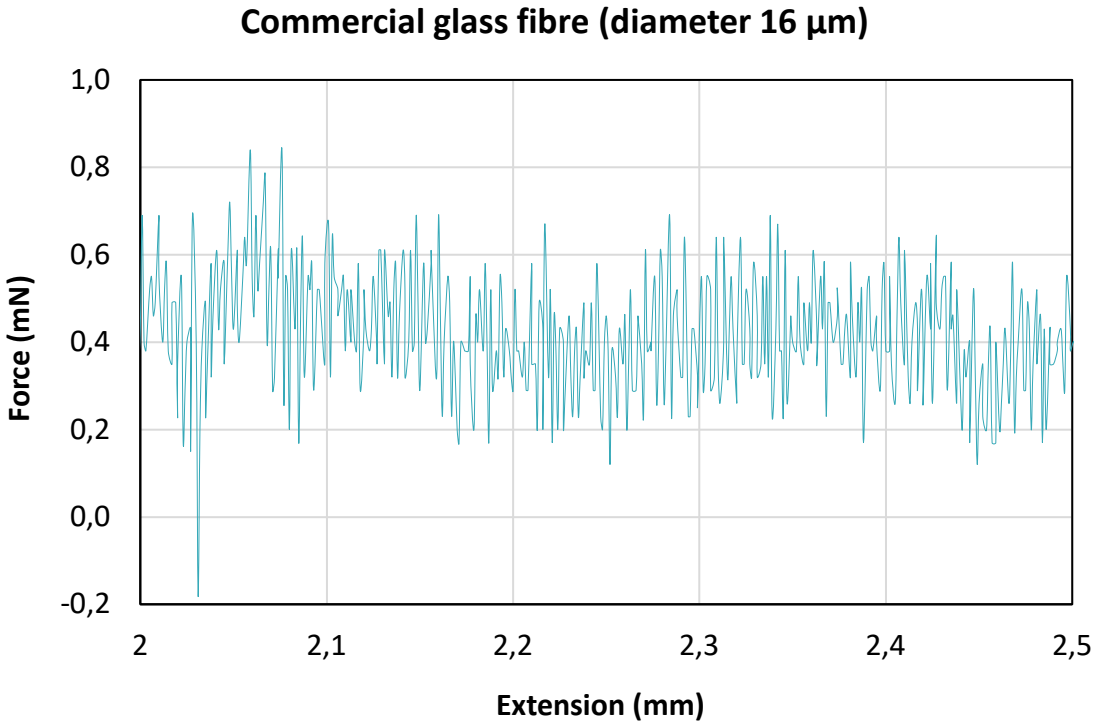

Figure 22: force-extension plot for peel test of SE3030 with VE-1260 at 90°

The peel force for these fibres was significantly lower; this is expected as the embedded perimeter is smaller and peeling was at 90° to the resin surface. A length of 10 mm was debonded during the test, from which a 0.5 mm segment is shown in Figure 22. Within this segment the peel angle was maintained at close to 90°. The average debonding force recorded was 0.42 mN: following Eq. 1 the fracture energy release rate was 8.4 J/m^2.

4.3 Results from DTU experiments

To study the proof of concept of the method described in section 3.4, two samples of VE1260/SE3030 were tested, with multiple videos taken per sample. The results of the fracture energy analyses are presented in Table 1. An assumed value of 70 GPa was used for the glass fibre stiffness **E** and the fibre radius was measured directly from the SEM images. All radii of curvature were obtained at a position 1 fibre diameter away from the crack tip (in the direction of the peel force in Figure 14).

The DACOMAT project has received funding from the European Union's Horizon 2020 research and innovation programme under GA No. 761072

For sample S3-02, fractures in the order of 10 times the fibre diameter were observed, whereas for sample S3-03 the fractures were much less pronounced (1 fibre diameter or less). This is reflected in a larger radius of curvature at fracture which resulted in a lower interfacial fracture energy. A number of factors may have influence on this result such as degree of cure and fixture travel speed.

Table 1: Interfacial fracture energy determined by in-situ SEM experiment.

Specimen ID	Material	Radius of curvature Rho (m)	Fibre radius r (m)	Fibre stiffness E (N/m2)	Interfacial fracture energy G_i_c (J/m2)
S3-02 VID02 - time=17:00	VE1260/SE3030	7.00E-04	8.075E-06	7.00E+10	9.40
S3-02 VID03 - time=33:36	VE1260/SE3030	5.82E-04	8.075E-06	7.00E+10	13.60
S3-02 VID03 - time=33:77	VE1260/SE3030	7.48E-04	8.075E-06	7.00E+10	8.23
S3-03 VID12 - time=05:21	VE1260/SE3030	1.23E-03	8.050E-06	7.00E+10	3.01
S3-03 VID13 - time=23:15	VE1260/SE3030	1.42E-03	8.050E-06	7.00E+10	2.28

At this stage it is difficult to make confident comparisons of the fracture energies calculated using the two different approaches to the single fibre peel test. Only a very small amount of data has so far been obtained for similar material systems. For these cases, fracture energies measured using in-situ SEM technique are within a similar range to the preliminary results using the fixed 90° angled stage with tensile machine. Results for the fixed 30° stage, however, are significantly higher; depending on which data from Table 1 are used for comparison the factor of the difference is between about 2-10. Some explanations for this have been identified.

1. Higher debonding force/fracture energy is expected for peeling at an oblique angle compared to normal to surface peeling. Therefore, data generated using in-situ SEM testing are expected to be slightly lower.
2. Samples peeled at oblique angle inspected post-test showed signs of significant residual resin. This may (a) increase the size of the debond region which was not accounted for in the calculation of interfacial fracture energy, or (b) mean that that the fracture energy measured was at least partly due to the creation of new interface within the near-interface polymer region.

The next planned experiments will produce a larger matrix of data to compare the 2 testing approaches. This will include fully sized SE3030 fibre, unsized glass fibre and steel wire and a range of vinyl ester resins and DER332 epoxy.

Observations/Discussion:

During the peeling experiment, the fibre was observed to slip from the movable stage (Figure 15), where it was held using carbon tape. Future experiments may use improved mechanical fastening to avoid such slippage.

Interpolation criteria used for curved section were not deemed to be robust enough for reliable comparison between different specimens. The selection of boundaries for the interpolation could result in factor 3 difference in interfacial fracture energy. It is suggested to use an interpolation function based on beam theory to avoid the use of piecewise interpolation of the straight and curved sections of the fibre.

The DACOMAT project has received funding from the European Union's Horizon 2020 research and innovation programme under GA No. 761072

Further experiments are required with updated interpolation methods and different material systems to prove this method for determining fibre/matrix interfacial fracture energy.

4.4 Comparison of results between DTU and UNIS test methods

Limited comparison can be made between results generated using the two techniques developed to carry out peel testing: either through measurement of debond force and embedded perimeter, or by SEM observation of the fibre's radius of curvature at the crack tip and embedded depth. Directly comparable results were presented in 4.2.3 and 4.3 for SE3030 fibres embedded in VE-1260 to approximately 50 % of their diameters.

A range of values of fracture energy of between 2.3 – 13.6 J/m^2 were calculated from observation of fibre radius of curvature at DTU. The preliminary value obtained from measurement of debonding force at UNIS was 8.4 J/m, which falls within this range. These initial results suggest there may be an acceptable degree of comparability between the test methods, however it is important to remember that these results are only preliminary and further testing is required.

Some comparison of these results with those of other researchers can be made. In their work on fibre peeling, Alimuddin and Piggott measured the work of fracture between and E-glass fibre (sizing not specified) and a low viscosity DGEBA based epoxy resin with n-butyl glycidyl ether. The value reported was 140 ± 50 J/m^2. This is more than an order of magnitude higher than the preliminary values in this report. It is not yet known why this difference is so large: data from mode II micromechanical test results suggest that the interfacial shear strengths are only slightly greater for epoxies than for vinyl esters.

Liechti and Chai [8] measured the toughness of glass/epoxy interfaces using edge-cracked bi-material strips of glass and epoxy. In the study there is no indication that a sizing agent was used to treat the glass prior to casting the epoxy layer onto it. The bi-material strips were loaded under a variety of mode mixities, ranging from pure bond-normal opening to pure bond-tangential opening. Interfacial fracture toughness was found to be 3 J/m^2 for bond-normal opening and up to 36 J/m^2 for bond-tangential opening.

The fracture toughness values obtained by UNIS (27.7 J/m^2) for a glass fibre/epoxy interface lies well within this range. However, the mode-mixity of the UNIS experiment must be determined for an accurate comparison. The fracture toughness values obtained by DTU (2.3-13.6 J/m^2) and UNIS (8.4 J/m^2) for a glass fibre/vinyl ester interface are also within the range described by Liechti and Chai.

4.5 Peel angles and mode mixitiy

Thouless and Jensen [9] analyzed the peel test and derived an equation for the mode mixity. They found that for indentical elastic properties of the film and substrate, the mode mixity was surprisingly insensitive to the peel angle in the range of 0 to 90 degrees. For identical film and substrate materials they found that the mode mixity to be approximately -38 degrees. The negative sign of the mode mixity phase angle indicates that the interface crack has a tendency to kink into the film, not into the substrate.

An independent estimate [10] estimates that the mode mixity of a fibre peeling off is in the range of 38 to 52 degrees.

The DACOMAT project has received funding from the European Union's Horizon 2020 research and innovation programme under GA No. 761072

Furthermore, a phase angle about 40 degrees is typically in the range of mode mixity where that mixed mode interfacial fracture energy is not varying significantly from the fracture energy of normal opening ("Mode I"), see e.g. Liechti and Chai [8] and Sørensen et al. [11] This suggests that a fracture energy correctly (e.g., measured from fibres that were not over-embedded) determined from a peel-off experiment should be well representative of the fracture energy of bridging fibres in a crack in a composite material, irrespective of the angle of the bridging fibres.

5.Summary and conclusions

A small number of micromechanical interface tests have typically been used to investigate adhesion of reinforcement fibres and polymer matrix materials in the literature. These tests are fibre micro droplet debond, single fibre fragmentation, fibre pull out and fibre push out. These tests cause failure by shear and the most commonly reported property is the interfacial shear strength (IFSS). Although they remain relatively common in the literature, criticisms of all these tests has been levelled regarding unrealistic centro-symmetric form of failure and the possible exaggerated effect on results of the fibre surface roughness and matrix cure shrinkage. An alternative, the single fibre peel test, was demonstrated but did not persist in the literature. The ideas behind this test have been revived and a new fibre peel test has been designed and trialled.

New methods of sample preparation have been investigated using flat substrates. It was demonstrated that resins with sufficiently low viscosity can be dispersed in a thin and relatively even film using spin coating. A layer of resin approximately 10 µm thick was achieved using a glass substrate. An alternative method of resin dispersal was also developed. Mechanical rolling of resin on a substrate produced a significantly thicker layer (greater than 0.1 mm). It also allowed the use of more viscous resins which cannot be dispersed by spin coating.

Surface profilometry was identified as a suitable technique to efficiently and accurately measure the embedded perimeter between a single fibre and the resin in which it was embedded. This technique can be used either before or after the debond is carried out, however it is more advantageous to do so post-test.

Two methods of single fibre peel test have been developed. A simple, low cost testing fixture was developed for single fibre peel testing at multiple angles, using a standard single column tensile machine with low capacity load cell. Fixed angle fixtures are 3D printed using PLA and affixed to a solid aluminium base using a dovetail. Initial experiments suggest that this test setup is effective and the data obtained are in somewhat line with expectations from previous studies. Refinement of sample preparation is required as initial results suggest that clean debonding at the fibre-matrix was not consistently achieved.

An environmental SEM with moveable stage was utilised for a second fibre peel test method. The substrate was fixed on one side of the stage and the free fibre end to the other. The test curvature of the fibre was recorded as the stage moved, progressively peeling the sample. An expression was developed such that fracture energy was calculated from crack tip curvature, and fibre radius and Young’s modulus.

Preliminary results suggest that both methods of testing and analysis have promise. The values of fracture energy are in a reasonable range based on previous literature. The level of agreement

The DACOMAT project has received funding from the European Union's Horizon 2020 research and innovation programme under GA No. 761072

between the two tests is good based on results produced thus far, but a more robust assessment with larger sample sizes and utilising a range of materials must be carried out.

References

[1] Sørensen BF. Micromechanical model of the single fiber fragmentation test. Mech Mater 2017;104:38–48. https://doi.org/10.1016/j.mechmat.2016.10.002.

[2] Piggott MR. Why interface testing by single-fibre methods can be misleading. Compos Sci Technol 1997;51:965–74.

[3] Piggott MR. Why the fibre/polymer interface can appear to be stronger than the polymer matrix. Compos Sci Technol 1997;57:853–7. https://doi.org/10.1016/S0266-3538(96)00151-0.

[4] Alimuddin MA, Piggott MR. Fracture Toughness of Fiber-Polymer Interfaces Estimated From Single Fiber Peel Tests. Polym Compos 1999;20:655–63.

[5] Alimuddin MA. Peel Test for the Evaluation of Environmental Effects on Fiber-Polymer Interface. University of Toronto, 1999.

[6] Sun J. Peel test for the study of the fibre polymer interface. University of Toronto, 2001.

[7] Toftegaard HL, Sørensen BF. General J integral solution for specimens loaded by moments, axial forces and residual stresses – A unifying stiffness formulation. Eng Fract Mech 2019;217:106500. https://doi.org/10.1016/j.engfracmech.2019.106500.

[8] Liechti KM, Chai YS. Asymmetric Shielding in Interfacial Fracture Under In-Plane Shear. J Appl Mech 1992;59:295–304. https://doi.org/https://doi.org/10.1115/1.2899520.

[9] Thouless MD, Jensen HM. Elastic fracture mechanics of the peel-test geometry, J. Adhesion, 1992;38:185-97.

[10] Sørensen BF, Gamstedt, EK, Østergaard R, Goutianos S. Micromechanical model of cross-over fibre bridging – Prediction of mixed mode bridging laws, Mechanics of Material, 2008;40:220-34.

[11] Sørensen BF, Jacobsen TK. Characterizing delamination of fibre composites by mixed mode cohesive laws, Composite Science and Technology, 2009;69:445-56.